

Deuterium chemistry of dense gas in the vicinity of low-mass and massive star forming regions

Zainab Awad^{1,2*}, Serena Viti², Estelle Bayet³, and Paola Caselli⁴

¹*Department of Astronomy, Space Science, and Meteorology, Faculty of Science, Cairo University, Giza 11326, Egypt*

²*Department of Physics and Astronomy, University College London, London WC1E 6BT, UK*

³*Sub-Department of Astrophysics, University of Oxford, Denys Wilkinson Building, Keble Road, Oxford, OX1 3RH*

⁴*School of Physics and Astronomy, University of Leeds, Leeds LS2 9JT, UK*

Accepted 2014 June 9. Received 2014 June 7; in original form 2013 October 8

ABSTRACT

The standard interstellar ratio of deuterium to hydrogen (D/H) atoms is $\sim 1.5 \times 10^{-5}$. However, the deuterium fractionation is in fact found to be enhanced, to different degrees, in cold, dark cores, hot cores around massive star forming regions, lukewarm cores, and warm cores (*hereafter*, hot corinos) around low-mass star forming regions. In this paper, we investigate the overall differences in the deuterium chemistry between hot cores and hot corinos. We have modelled the chemistry of dense gas around low-mass and massive star forming regions using a gas-grain chemical model. We investigate the influence of varying the core density, the depletion efficiency of gaseous species on to dust grains, the collapse mode and the final mass of the protostar on the chemical evolution of star forming regions. We find that the deuterium chemistry is, in general, most sensitive to variations of the depletion efficiency on to grain surfaces, in agreement with observations. In addition, the results showed that the chemistry is more sensitive to changes in the final density of the collapsing core in hot cores than in hot corinos. Finally, we find that ratios of deuterated sulphur bearing species in dense gas around hot cores and corinos may be good evolutionary indicators in a similar way as their non deuterated counterparts.

Key words: Astrochemistry - Stars: low-mass, massive, formation - ISM: abundances, molecules

1 INTRODUCTION

Observations of local interstellar deuterated molecules have long been used to probe the physical conditions within interstellar clouds. Although the interstellar ratio of deuterium to hydrogen (D/H) atoms within the Milky Way is only $\sim 1.5 \times 10^{-5}$ (Linsky et al. 1995; Oliveira et al. 2003), the observed degree of deuterium fraction¹ is enhanced in many astrophysical regions such as cold, dark cores (e.g. Tiné et al. 2000; Crapsi et al. 2005), hot cores around massive star forming regions (e.g. Ehrenfreund & Charnley 2000; Fontani et al. 2008), lukewarm cores (Sakai et al. 2009), and hot corinos around low mass star forming regions (e.g. Ceccarelli et al. 1998, 2001, 2007).

Although there are only few detections of HD, the simplest deuterated species (e.g. Wright et al. 1999; Bertoldi

et al. 1999; Polehampton et al. 2002; Caux et al. 2002; Neufeld et al. 2006; Yuan et al. 2012; Bergin et al. 2013), there is a growing body of observations, towards low- and high- mass star forming regions, for mono- as well as multiply deuterated species, such as H_2D^+ (e.g. Stark et al. 1999, 2004; Pillai et al. 2012), DCN (e.g. Wilson et al. 1973; van Dishoeck et al. 1995), HDO (Henkel et al. 1987; van Dishoeck et al. 1995), and DCO^+ (Penzias 1979; Butner & Loren 1988). The first detection of a doubly deuterated species (D_2CO) was towards Orion KL by Turner (1990). The same molecule was then detected towards the low-mass protostar IRAS16293-2422 (Ceccarelli et al. 1998) with a $\text{D}_2\text{CO}/\text{H}_2\text{CO}$ ratio 15 times higher than that obtained for Orion.

To-date, around 32 deuterated species have been detected in a variety of interstellar clouds including ND_3 , CHD_2OH , CD_3OH , D_2S , D_2O , HD_2^+ , CH_2DOH , H_2D^+ , C_3D , C_4HD , DC_5N , and DCOOCH_3 (e.g. see reviews Ceccarelli et al. 2007; Herbst & van Dishoeck 2009; Caselli & Ceccarelli 2012; Tielens 2013 and references therein). Ta-

* E-mail: zma@sci.cu.edu.eg

¹ The deuterium fraction is the abundance ratio of a molecule containing a deuterium atom (XD) to the equivalent molecule with a hydrogen atom (XH). Deuterium fractionation is the process which leads to the enhancement of the deuterium fraction.

Table 1. List of observed deuterated species in massive ‘H’ and low-mass ‘L’ star forming regions and the corresponding references.

Species	Region	Ref (e.g.)
H_2D^+	H	Pillai et al. (2012)
	L	Stark et al. (1999)
N_2D^+	H	Fontani et al. (2006)
	L	Emprechtinger et al. (2009)
DCO^+	H	Penzias (1979)
	L	Butner & Loren (1988)
CH_2D^+	H	Roueff et al. (2013)
DCN	H	Wilson et al. (1973)
	L	van Dishoeck et al. (1995)
$^\dagger \text{DNC}$	H	Rodgers & Millar (1996)
	L	van Dishoeck et al. (1995)
HDS	L	van Dishoeck et al. (1995)
D_2S	L	Vastel et al. (2003)
HDCO	H	Loren & Wootten (1985)
	L	van Dishoeck et al. (1995)
D_2CO	H	Turner (1990)
	L	Ceccarelli et al. (1998)
CH_3OD	H	Saito et al. (1994)
	L	Parise et al. (2002)
CH_2DOH	H	Jacq et al. (1993)
	L	Parise et al. (2002)
CHD_2OH	L	Parise et al. (2002)
CD_3OH	L	Parise et al. (2004)
C_2D	H	Vrtilek et al. (1985)
	L	van Dishoeck et al. (1995)
C_3D	L	Sakai et al. (2009)
C_4D	L	Sakai et al. (2009)
C_3HD	L	Sakai et al. (2009)
DC_3N	L	Sakai et al. (2009)
DC_5N	L	Sakai et al. (2009)
NH_2D	H	Rodriguez Kuiper et al. (1978)
	L	Shah & Wootten (2001)
ND_3	L	van der Tak et al. (2002)
HDO	H	Henkel et al. (1987)
	L	van Dishoeck et al. (1995)
D_2O	H	Neill et al. (2013a)
	L	Butner et al. (2007)
CH_2DCN	H	Gerin et al. (1992)
DCOOCH_3	L	Demyk et al. (2010)

 † Data for massive star forming regions ‘H’ is taken from Table 1 in Rodgers & Millar (1996)

ble (1) lists the observed deuterated species in cores around massive (H) and low-mass (L) star forming regions only.

In parallel to observational studies, theoretical modelling of deuterium chemistry has also been taken place over the years. Early attempts at studying deuterium chemistry used simple gas-phase models (Watson 1980) or surface chemistry (Tielens 1983). Both models were relatively successful in reproducing the observed deuterated species, at that time, and showed the role of grain surface reactions in enhancing deuteration of some species such as H_2CO . The first gas-grain chemical models were later developed by Brown & Millar (1989a,b). They found that surface chemistry can produce small but significant amounts of multi-deuterated molecules. Following this study, Millar et al. (1989) used a detailed numerical pseudo-time-dependent gas-phase chemical model to study deuteration in dense clouds. Their results showed that in cold clouds (~ 10 K)

the main sources of fractionation are H_2D^+ and its daughter ions DCO^+ and H_2DO^+ , while for warmer regions, up to 70 K, CH_2D^+ , C_2HD^+ , and associated species led to the high fractionation. The methodology of extending chemical networks to include deuterium was presented by Rodgers & Millar (1996) in their model of the deuterium chemistry in hot cores. They based their approach on the assumption that both H- and D-bearing species react with the same species with the same rate coefficient. Where there is an uncertainty, statistical branching ratios were assumed. Their model showed that the deuterium fractionation would be preserved in hot cores for at least 10^{4-5} yrs after evaporation. Following Rodgers & Millar (1996), Roberts & Millar (2000a,b) developed new chemical models including, for the first time, the deuterated sulphur-bearing species and gas-phase chemistry of some doubly-deuterated species to investigate the influence of varying a wide range of physical parameters on the fractionation in interstellar clouds. They found that the fractionation ratios are temperature and fractionation process (i.e. due to H_2D^+ , CH_2D^+ or C_2HD^+) dependent. In addition, they showed that H_2S and HDS are good probes for regions where grain surface chemistry is important. They also commented that HDCO and D_2CO are good probes for fractionation on grain surfaces. The detection of multiply deuterated isotopologues of H_3^+ (e.g. Caselli et al. 2003; Vastel et al. 2004) motivated Roberts et al. (2003, 2004) to release a new version of their model in which multiply deuterated isotopologues of H_3^+ are taken into account. Their results revealed that the inclusion of D_2H^+ and D_3^+ enhances the fractionation of ionic and neutral species because it allows more deuterium to transfer to other species in dark clouds. In addition, experimental work and chemical models showed that, in cold environments, the spin state of species (ortho, para, meta) affects the deuterium fractionation (e.g. Gerlich et al. 2002; Walmsley et al. 2004; Flower et al. 2006; Hugo et al. 2009; Sipilä et al. 2010), by allowing ortho- H_2 to react with deuterated isotopologues of H_3^+ and reducing deuterium fractionation.

It is clear that deuterium fractionation is a function of the chemical as well as the physical conditions of star forming regions. This paper is dedicated to investigate, theoretically, whether the evolution of deuterium chemistry differs significantly between low- and high-mass star forming regions by modelling deuterium chemistry under physical conditions likely similar to those of hot cores and corinos. Our model treats the desorption of the species, deuterated and non-deuterated, to be temperature dependent during the protostellar phase (the warming up phase). This approach allows for better identification of chemical tracers for various evolutionary stages in regions where the proto-star has started to affect the surrounding gas and dust.

The present model, UCLDCHEM, is an adaptation of the UCLCHEM model (Viti & Williams 1999; Viti et al. 2004), which in its original form did not include a deuterium network.²

This paper is organized as follows: in §2 we describe our model; in §3 we present the results of the grid of models we

² This paper is an extension with several updates to the original, unpublished, study performed by Zainab Awad as part of her Ph.D; see Awad (2010).

ran. We compare our model calculations with observations and other models in §4, and give our conclusions in §5.

2 THE MODEL

We have used a time-dependent gas-grain chemical model described in details in Viti et al. (2004) and Awad et al. (2010). The model is a two-phase code. The first phase (Phase I) simulates the free-fall collapse of a core as described in Rawlings et al. (1992). It starts with diffuse, mainly atomic material which has an initial number density of $\sim 400 \text{ cm}^{-3}$ and temperature of 10 K. The material undergoes a free-fall collapse up to a given final density considered here as a free parameter. During phase I, gas-phase chemistry and freeze-out on to grain surfaces occur. Accreted atoms and molecules hydrogenate or deuterate when possible. The depletion (or freeze-out) efficiency is determined by the amount of the gas-phase material frozen onto the grains. Since CO is the most abundant species, after H_2 , and because its depletion percentage is an important factor in measuring the deuterium fractionation (e.g. Caselli et al. 2002; Bacmann et al. 2003), we based our calculation of the depletion efficiency on the abundance of CO species. The depletion efficiency is regulated by varying the sticking probability of gas-phase species onto grain surfaces (Rawlings et al. 1992). In Phase II, we follow the chemistry of the remnant core, after the star is born. In this phase, the central star heats up the surrounding gas and dust, causing selective sublimation of the icy mantles. We adopt an identical treatment for the time dependent ice sublimation to Viti et al. (2004).

In this work, we have extended the species set used in Awad et al. (2010) by including all the possible mono-deuterated counterparts for H-bearing species to model deuterium chemistry. The only doubly deuterated species included in this model is D_2CO and its parent ion HD_2CO^+ . The exclusion of other doubly-deuterated species, as well as triply-deuterated species is of course a limitation of this model. However we note that the aim of this work is to characterize the general trends of the chemical evolution of hot cores and corinos (hence gas at temperature higher than 100K). In these warm regions deuteration is not as efficient as in dark clouds. The deuteration process is driven by H_2D^+ , C_2HD^+ and/or CH_2D^+ ions that are formed via radiative association reactions involving H_3^+ , C_2H_2^+ , and CH_3^+ ions, respectively. At low temperatures, H_3^+ is the most abundant ion and hence fractionation of H_2D^+ is the most important of the three. At temperatures higher than 25K, however, H_2D^+ is destroyed by H_2 . CH_2D^+ and C_2HD^+ are important for deuteration in regions colder than 60 and 80 K, respectively (Millar et al. 2000; Parise et al. 2009). Hence, the amount of doubly and triply deuterated forms of H_3^+ or CH_3^+ should be negligible at temperatures higher or equal to 100K. While therefore our chemistry is limited during Phase I (leading to the warm up phase starting with a deuteration fraction that may not be as accurate) by focusing on the trends during the warm up phase, in the warm gas, a slightly lower or higher deuteration at the beginning of Phase II should not affect the trends. In fact chemical models by Roberts et al. (2003) revealed that the inclusion of multiply deuterated forms of H_3^+ improved the results for

certain ions, namely N_2H^+ . Our model supports this result (see Section 3).

Our chemical network is based on the network previously described by Roberts & Millar (2000a). However, we updated several reactions following Woodall et al. (2007)³ ratefile and using Rodgers & Millar (1996) recipe in generating the reactions involving the deuterium counterparts. Moreover, the rate coefficients for some radiative association reactions and the binding energies for surface species were also updated following Roberts et al. (2004) and Roberts & Millar (2007), respectively. Beside these updates, we included all the freeze-out reactions for hydrogen bearing species and their deuterium counterparts, assuming that the products will have the same branching ratios adopted for their hydrogen equivalents. The surface chemistry considered here is simple in that it includes, besides the H_2 and HD formation on grains, rapid hydrogenation of species, where energetically possible. Apart from direct hydrogenation, the only other surface reactions we include are the formation of methanol from CO and of CH_3CN from the reaction of methane, CH_4 , with HCN, as it has been shown that gas phase reactions are not sufficient to form these two species (e.g. Tielens & Hagen 1982; Watanabe et al. 2003; Garrod et al. 2008). As a first approximation and according to experimental results of the thermal desorption non-deuterated species from icy mantles (e.g. Collings et al. 2003a, 2004), we assumed that deuterated species will desorb at the same temperature recorded for their hydrogen counterparts (*McCoustra - private communication*). Desorption temperatures are listed in Table (2) in Viti et al. (2004) for hot cores and determined by Awad et al. (2010) for hot corinos.

This work studies the influence of changing the final density of the collapsing core, the depletion efficiency of the gaseous species onto grain surfaces, and the effect of varying the collapsing mode (free fall or retarded)⁴ on the chemical evolution of deuterated species around low-mass (1 M_\odot) and higher mass ($5 \text{ \& } 25 \text{ M}_\odot$) protostars.

In the first instance, we ran a total of 9 models, where the initial elemental abundances and parameters used for the grid are listed in Tables (2) and (3). Our chemical network consists of 265 species (including 92 deuterated species and 60 surface species) linked in 4204 reactions both in gas-phase and on grain surfaces.

3 RESULTS AND DISCUSSION

We investigate the sensitivity of deuterium chemistry to changes in the physical conditions in low- and high-mass star forming regions by comparing the reference models M1, M4 and M7 (for masses: 1, 5, and 25 M_\odot ; respectively - see Table (3)) to the following models: M2, M5, and M8 to study the influence of changing the final density of the collapsing cloud; and models: M3, M6, and M9 to explore

³ This work was performed before the release of the UMIST 2012 ratefile (McElroy et al. 2013).

⁴ A retarded collapse means that the speed of the collapse is a factor of that of the free-fall collapsing speed which we assume it is unity. In this model we change the speed of the collapse by varying the collapse parameter defined in the modified collapse equation by Rawlings et al. (1992).

Table 2. Initial elemental abundances, with respect to the total number of hydrogen nuclei, and physical conditions assumed in our model (taken from Viti et al. 2004; Awad et al. 2010). Note that for the described parameters, hereafter, the temperature is the gas kinetic temperature (in K) and the density is the gas number density (in cm^{-3}).

Initial elemental abundances		
Carbon	1.79×10^{-4}	
Oxygen	4.45×10^{-4}	
Nitrogen	8.52×10^{-5}	
Sulphur	1.43×10^{-6}	
Helium	7.50×10^{-2}	
Magnesium	5.12×10^{-6}	
Physical parameters		
The parameter	Hot Corino Awad et al. (2010)	Hot Core Viti et al. (2004)
† Core density (cm^{-3})	$10^7 - 10^8$	$10^6 - 10^7$
Core temperature (K)	100	300
Core radius	150 AU	0.03 pc
Protostellar Mass (M_{\odot})	1	5 & 25
	<u>For Both Models</u>	
† Depletion percentage (%)	85 - 100	
† The collapsing mode	free fall - retarded	

[†] This parameter varies only during the collapsing phase (Phase I).

Table 3. Summary of the grid of our models in this study as described in §3

Models	Mass M_{\odot}	Temperature K	[†] Density cm^{-3}	[†] Depletion %
M1	1	100	2.0×10^8	100
M2	1	100	1.0×10^7	100
M3	1	100	2.0×10^8	85
M4	5	300	1.0×10^7	100
M5	5	300	1.0×10^6	100
M6	5	300	1.0×10^7	85
M7	25	300	1.0×10^7	100
M8	25	300	1.0×10^6	100
M9	25	300	1.0×10^7	85
*Models with different collapse speeds				
Models	speed of collapse	Notes		
ff	1	free-fall collapse with assumed speed unity.		
ret 0.5	0.5 ff	retarded collapse with half the speed of the ff model.		
ret 0.1	0.1 ff	retarded collapse with tenth the speed of the ff model.		

M1, M4 and M7 are the reference models in the grid.

[†] These parameters vary only during the collapsing phase (Phase I) of the chemical model.

* These models have similar physical conditions to that of model M1. ff: free-fall collapse model, ret: retarded collapse model

the influence of varying the depletion percentage of gaseous species onto grain surfaces. Note that the mass in the second column is that of the newly formed star. The influence of changing the final density of the collapsing core and the depletion efficiency were studied by adopting some standard values - see Table (3) - and then decreasing their values by 10 and 15%, respectively. The standard values are listed in Table (3): model M1 for a solar mass hot corino and models M4 and M7 for 5 and 25 solar masses hot cores. The choice of these values is arbitrary providing that the model physical conditions are within the observed ranges for low- and

high- mass cores. Figs. (1 - 4) show the predicted fractional abundances as a function of time for hot corinos (panel a) and hot cores (panels b and c).

The effect that the collapse timescale may have on the chemistry has been previously discussed for low-mass stellar cores by Sakai et al. (2008). Hence here we focus on the influence of varying this collapse timescale for hot corinos only: We compare models ‘ret 0.5’ and ‘ret 0.1’ to the standard ‘ff’ model of a hot corino to understand the impact of varying the speed of the collapse on the chemical timescales of the region under study. Fig. (5) illustrates the fractional

abundances of species in a hot corino as a function of time for free-fall (solid line) and retarded collapse (dashed and dotted line) models.

3.1 Sensitivity to the final core density

Generally, a change in densities affects hot corinos more than hot cores. This result is shown in panels (a), (b) and (c) in Figs. (1) and (2). These figures represent Models M1(M2), M4(M5), and M7(M8), when the final density is $10^8(10^7)$ cm^{-3} for hot corinos, and $10^7(10^6)$ cm^{-3} for hot cores.

As expected, species in hot corinos are more abundant in denser cores (solid line) than in less dense cores (dashed line); exceptions are CH_3OD , CH_2DOH , and HDO that show higher abundances for less dense regions, in particular during early times ($t \leq 10^5$ yrs). Generally, the two deuterated methanol counterparts show the same evolutionary profile, but CH_3OD seems to survive longer than CH_2DOH . The chemical analysis of those species, in dense regions (10^8 cm^{-3}) at early times, reveals that they are destroyed via reactions with H^+ that are more efficient at higher densities. Therefore, their abundances remain high for longer times in less dense regions. For both models, M1 and M2, HDO is formed via reactions involving H_2CO (see next section) which are more efficient at lower densities (Model M2). The abundance of HDO is enhanced for times $\geq 10^5$ yrs, which is consistent with the desorption times of H_2CO from grain surfaces in the H_2O co-desorption event (Awad et al. 2010). Moreover, the number of destruction pathways of heavy water in denser cores is larger than that for less dense cores, allowing more HDO to remain in the gas-phase.

All the species experience a rapid and steeper decline in their abundances in less dense (10^7 cm^{-3}) hot corinos (Panel a) than in denser ones (10^8 cm^{-3}). The chemical trends in the two models remain the same except for HDCO , which shows fluctuations in its abundance for low density hot corinos, in particular after 10^5 yrs. The chemical analysis of HDCO at this particular time for a lower density hot corino reveals that the species is involved in a larger number of gas-phase reactions than in the case of a denser core.

Molecules in massive cores (with higher temperature) are less affected by the decrease in core density. However, deuterated water shows a slightly higher abundance at times $\leq 2 \times 10^5$ yrs, and both forms of deuterated methanol are less abundant in lower density cores.

3.2 Impact of varying the depletion efficiency

Observations reveal that the enhancement of the deuterated species to their fully hydrogenated forms arises in regions where the CO molecules are heavily depleted onto dust grains (e.g. Caselli et al. 2002; Bacmann et al. 2003; Millar 2005; Crapsi et al. 2005; Chen et al. 2011). Therefore, we studied the influence of varying the depletion percentage on the fractional abundances of the species in hot corinos and cores.

In this section, we discuss the results of modelling hot corinos and cores with fully (Models M1, M4, & M7) and partially depleted gas (Models M3, M6, & M9), respectively. The chemical evolution of deuterated molecules in a fully depleted gas (solid line) is plotted in comparison with the

case of partially depleted gas (dashed line), both as a function of time, in Figs (3) and (4). The term ‘fully depleted’ refers to interstellar gas which is close to 100% freeze-out by the end of the collapsing phase (Phase I), while ‘partially depleted’, in this paper, means an arbitrary freeze out percentage of $\sim 85\%$. Generally, models with partially depleted gas yield lower abundances for all deuterated species, apart from HDCS which is enhanced between 9×10^4 yrs and ~ 1 million years. In massive cores, and for times earlier than 1.6×10^5 yrs, the fractional abundances of HDO , D_2CO , and the two deuterated forms of CH_3OH show a slight enhancement with lower depletion percentage. The abundance of HDS is the least affected by a lower depletion percentage. This is probably due to the fact that HS and its deuterated counterpart are not formed or enhanced on the icy mantles. Chemical analysis of HDCS reveals that prior to 9×10^4 yrs, the formation rate of HDCS is similar in both models while after that time, and when mantle species sublime, the formation rate of HDCS increases in models with partial depletion. This result may indicate that this molecule is mainly formed via gas-phase reactions and is not a mantle species. HDO , in hot corinos (Fig. 3, panel a), with higher depletion percentage (solid line) shows higher abundances at late times. At times of $\sim 1.7 \times 10^4$ yrs, the abundance of HDO shows a sudden increase which cannot be explained in terms of mantle sublimation. The chemical analysis at the time around this ‘jump’ reveals that it is caused by the presence of methane (CH_4) in the gas phase. The time of the ‘jump’, $\sim 1.7 \times 10^4$ yrs, is associated with that observed previously for formaldehyde (Awad et al. 2010). In this model, HDO is produced via reactions involving H_2CO or HDCO with H_2DO^+ . As a consequence, we argue that the increase in the HDO abundance can be explained as a result of the enhancement in the formation of either H_2CO or HDCO , as follows. CH_4 evaporates from grain surfaces at $\sim 1.7 \times 10^4$ yrs, then it undergoes many gas-phase reactions some of which form H_2DO^+ and CH_3 . These two molecules are, in turn, used to form H_2CO and HDCO leading to an enhancement in their abundances. Therefore, the jump of HDO can be attributed, indirectly, to the evaporation of methane from grains surfaces.

On the other hand, D_2CO is enhanced in hot corino models with full depletion. This result is supported by Bacmann et al. (2003), see Section (4). In hot cores, the deuterated forms of H_2CO and CH_3OH (Fig. 4) for both models are abundant for longer times than in hot corinos and hence these species may be good tracers of hot cores. For earlier times (i.e. $t < 10^4$ yrs), deuterated H_2CO and CH_3OH (mainly formed on grains) can be formed, in the gas phase, via reactions involving HCN (e.g. $\text{H}_2\text{DCO}^+ + \text{HCN} \rightarrow \text{HCNH}^+ + \text{HDCO}$) and NH_3 (e.g. $\text{CH}_3\text{OHD}^+ + \text{NH}_3 \rightarrow \text{NH}_4^+ + \text{CH}_3\text{OD}$).

Unlike the case of hot corinos, D_2CO is observable in hot cores even when the depletion percentage is low. This molecule is efficiently formed via the reaction ‘ $\text{HD}_2\text{CO}^+ + \text{H}_2\text{O}$ ’, and is destroyed by H_3O^+ and HCO^+ . The latter dominates the destruction routes at times later than 1.4×10^4 yrs, but it is less efficient in hot core models with partial freeze out, leading to a higher D_2CO abundance. HDCO is abundant during most of the hot core lifetime and therefore could be used as a good tracer for hot cores. It is interesting to note that HDCO shows a sudden increase in its

abundance, even at low depletion efficiencies, around 4×10^4 yrs, which cannot be explained by its sublimation from grain mantles (as in the hot corinos case). This ‘jump’ in abundance is related to the formation of CH_4 , as explained above for hot corinos, but in hot cores H_2CO is mainly formed via oxidization reactions of CH_3 , which is formed via the efficient destruction of CH_4 .

DCN is another species that seems to be affected by the degree of depletion in Phase I; Parise et al. (2009) observed and modelled the excitation of HCN and DCN in Clump 1 and 3 of the Orion Bar and estimated the DCN/HCN ratios, on average, to be 0.7 and 1.1 (using the rotational diagram method) or 0.3 and 0.8 (using the LVG analysis), respectively. Our model calculations are in the range determined by Parise et al. (2009) and indicates that, in general, fully depleted cores have a lower deuterium fraction ($\sim 0.1 - 0.7\%$) than partially depleted cores ($\sim 0.8 - 1.2\%$). A chemical analysis shows that the rate of formation of DCN is higher in regions with full depletion compared to those with partial depletion. The reason for this is that for less depleted cores, DCN formation is mainly via the reaction ‘ $\text{NH}_3 + \text{DCNH}^+$ ’ which is inefficient in fully depleted cores. Moreover, DCN is extensively destroyed by the ion ‘ N_2H^+ ’ in cores with fully depleted gas. This route is of equal weight with other destruction pathways in cores with partially depleted gas. Our results for fully depleted models are consistent with those obtained for Clump 1 while partial depletion results are in better agreement with the observed values in Clump 3. Our modelling suggest that the percentage of the DCN/HCN molecular ratio can be used to trace the initial level of depletion (i.e. before the protostar switches on) in a given region.

3.3 Sensitivity to the mode of collapse

In their study of the chemistry of the low-mass core IRAS 04368+2557 in L1527, Sakai et al. (2008) concluded that the timescale of the collapse of the pre-stellar core affects the abundances of the species in the region under study. The shorter the timescale (i.e. the faster the collapse) the more abundant the species are, in particular C-bearing species (C_nH_m). This result motivated us to run two extra models for a solar mass core in which we vary the speed of the collapse in Phase I. The results are then compared to those of a standard solar mass hot corino (Model M1 in this work which undergoes a free-fall collapse), see the parameters of Model M1 and other models in Table (3). Models with longer collapse timescale (e.g. Model ret 0.1) are expected to form more species than models with shorter collapse timescale (e.g. Model M1), and therefore show an enhancement in the fractional abundances of their molecular content in Phase II.

Figure (5) shows the chemical evolution of the deuterated species during Phase II, for the free fall (solid line) and the retarded collapse models in which the speed of the collapse was decreased to half (dashed line) and a tenth of its free fall value (dotted line). From this figure, we note that when species are evaporated from the grain surfaces (after $\sim 4.8 \times 10^4$ yrs): (1) the least affected species by changing the mode of collapse are HDS and HDCO, and (2) the fractional abundance of HDCS and D_2CO decrease while that of the rest of the species increases as the speed of the col-

lapse decreases. The most affected species, and hence possible good indicators of the collapsing mode, are HDCS, NH_2 , CH_2DOH , and HDO. We conclude that $\text{HDO}/\text{H}_2\text{O}$ is affected by the collapse history of the pre-stellar core.

Our results are in agreement with the findings of (Sakai et al. 2008) in which the affected species in models with longer collapse timescale (Model M1 - solid line) possesses the lowest abundance of all models. We hence conclude that the speed of the collapse influences the fractional abundances of hot corinos.

3.4 Evolutionary stages indicators

Viti et al. (2004) studied the chemical evolution of hot cores around stars with various masses from 5 to 60 solar masses. They found that ratios of sulphur bearing species (e.g. $\text{H}_2\text{S}/\text{SO}_2$, $\text{H}_2\text{S}/\text{CS}$, SO/CS) are good indicators of the early stages of massive star formation while large organic molecules such as CH_3OH , HCOOCH_3 , and $\text{C}_2\text{H}_5\text{OH}$ indicate late evolutionary stages. In this work, we aim to investigate whether the deuterated counterparts of these evolutionary indicators can also be used for the same purpose. We, therefore, ran a grid of four additional models to cover the range of stellar masses between 10 and 60 solar masses (as in Viti et al. 2004). Fig. (6) illustrates the chemical evolution of sulphur bearing species and their deuterium counterparts. Inspection of this figure shows that, as their non-deuterated counterparts, the ratios of deuterated sulphur bearing species may be good chemical evolutionary tracers of hot cores in all cases explored.

4 COMPARISON WITH OBSERVATIONS AND OTHER MODEL CALCULATIONS

We briefly discuss our results by qualitatively comparing them to one representative hot corino and one hot core in §4.1, and by comparing our models with previous chemical modelling in §4.2.

4.1 Comparison with Observations

Our physical conditions for models of hot corinos (model M1) are comparable to those observed for the IRAS 16293-2422 source, while those of hot cores (model M7) are close to observations of Orion KL hot core. Hence we briefly compare our results with the observed abundances of these two sources.

IRAS 16293-2422 is a nearby Class 0 protostar at distance ~ 120 pc and predicted age of 10^5 years (André et al. 1993). It has an inner small (150 AU) condensed ($\sim 2 \times 10^8 \text{ cm}^{-3}$) region known as ‘hot corino’ (Ceccarelli et al. 1998). A comparison between Model M1 fractional abundances and the calculated molecular D/H ratios of various species with those derived from observations of IRAS 16293-2422 source and the times of best fit of our calculations with observations are summarized in Table (4). All of our fractional abundances are given relative to the total number of H nucleons in the region. Note that for most observations quoted in Table (4) we cannot distinguish the emission from the inner hot corino region and that from the external outer region of the

Table 4. Comparison between observations of deuterated species and molecular D/H ratios in the IRAS 16293-2422 hot corino source and our model M1 calculations of Phase II.

Species	Observations	This Work M1	Time of best fit yrs	Ref
DCO⁺	7.5(-12)	~1 - 5(-11)	≤9.00(3)	van Dishoeck et al. (1995)
DCN	1.3(-11)	1.3 - 5.7(-10)	1.7 - 9(4)	van Dishoeck et al. (1995)
DNC	2.5(-12)	≤1(-13)	all times	van Dishoeck et al. (1995)
HDS	7.5(-11)	1(-7) - 1(-10)	6(4) - 2.5(5)	van Dishoeck et al. (1995)
HDO	9(-8)	≤1(-7)	all times	Coutens et al. (2013)
NH₂D	5(-10)	4(-8) - 1(-10)	9(4) - 9(5)	van Dishoeck et al. (1995)
HDCO	6(-11)	≤6(-11)	1.8(4) & ≥2.5(5)	van Dishoeck et al. (1995)
		≥6(-11)	0.17 - 2.5(5)	
[†] D₂CO	5(-10)	~4(-10)	0.2 - 2.4(5)	Ceccarelli et al. (1998)
[†] CH₃OD	3.6(-10)	≤4(-11)	0.9 - 5.7(5)	Parise et al. (2002)
[†] CH₂DOH	7.5(-9)	≤9(-11)	1.4 - 3.5(5)	Parise et al. (2002)
C₂D	2.3(-11)	1 - 4.5(-11)	3.8 - 5.5(4)	van Dishoeck et al. (1995)
[†] DCOOCH₃	1.5(-9)	≤1(-13)	all times	Demyk et al. (2010)
Ratio				
DCO⁺/HCO⁺	0.009	0.009	~ 4.03(4)	van Dishoeck et al. (1995)
DCN/HCN	0.013	0.012	2.6(4)	van Dishoeck et al. (1995)
DNC/HNC	0.03	≤1(-7)	all times	van Dishoeck et al. (1995)
C₂D/C₂H	0.18	0.18	4.7(4)	van Dishoeck et al. (1995)
HDCO/H₂CO	~0.14	few(-1)	2(3) - 1.6(4)	Roueff et al. (2000)
D₂CO/H₂CO	≤0.1	≤0.1	≥1.7(4)	Ceccarelli et al. (1998)
D₂CO/HDCO	≤0.5	≤0.5	1.8(4) - 1.32(5)	Roueff et al. (2000)
NH₂D/NH₃	~0.1	≤1(-4)	all times	Roueff et al. (2000)
HDO/H₂O	0.04 - 0.51	1 - 2	all times	Coutens et al. (2013)
CH₃OD/CH₃OH	0.02	≤0.1	≥ 1.74(4)	Parise et al. (2004)
CH₂DOH/CH₃OH	0.30	1-9(-1)	≥ 1.74(4)	Parise et al. (2004)
HDS/H₂S	0.1	0.15±0.01	6.9 - 9.1(4)	van Dishoeck et al. (1995)
[‡] N₂D⁺/N₂H⁺	0.25	≤0.25	all times	Roberts & Millar (2007)

[†] This value is converted into fractional abundance assuming $N(\text{H}_2) = 2 \times 10^{23} \text{ cm}^{-2}$ as given by van Dishoeck et al. (1995).

a(b) means $a \times 10^b$

[‡] Ratio observed in NGC 1333 IRAS4 by Roberts & Millar (2007)

source; an exception is the deuterated water observations by Coutens et al. (2013).

Most of the species in our sample match observations at times between 10^4 and 10^5 years, which is the assumed age for a typical Class 0 source (André et al. 1993). Exceptions are the ions that fit observations at times earlier than 10^4 years and show a rapid decrease after that time, and HDO that does not match observations at any time and is always underestimated by our model.

Deuterated ammonia matches observations at times later than 9×10^4 years. Currently, our model is underestimating the abundances of some deuterated species by one or two orders of magnitude, such as CH_3OD , CH_2DOH , DNC , and DCOOCH_3 . The main reason for this is perhaps the exclusion of multiply deuterated H_3^+ isotopologues that play a role in enhancing the deuterium fractionation via gas-phase chemistry (Roberts et al. 2003).

The $\text{N}_2\text{D}^+/\text{N}_2\text{H}^+$ ratio matches observations only during early times $\sim 4 \times 10^3$ years. In fact, Roberts & Millar (2007) surveyed the $\text{N}_2\text{D}^+/\text{N}_2\text{H}^+$ ratio around a sample of Class 0 sources and concluded that the high ratio observed represents the cooler gas in the extended envelope around the source and not the hot gas in the core. Similar results were reported by Emprechtinger et al. (2009) in their survey for $\text{N}_2\text{D}^+/\text{N}_2\text{H}^+$ in a sample of Class 0 sources. Yet our cal-

culated $\text{HDO}/\text{H}_2\text{O}$ ratio does not match observations. This must be because our model underestimates the fractionation by at least a factor of two which could be a result of our model limitations, described earlier in §2.

The Orion Kleinmann-Low nebula (Orion KL) is the nearest massive star-forming region at ~ 410 pc. The core has physical conditions ($n(\text{H}_2) = 10^7 \text{ cm}^{-3}$, $T \sim 150$ -300K, mass $\sim 15 M_\odot$; see Neill et al. 2013a; Kaufman et al. 1998 and references therein) close to those of our model M7. Most recently, Neill et al. (2013a,b) surveyed deuterated molecules in the Orion KL region using the Herschel/HIFI facilities. Table (5) summarizes a comparison between fractional abundances **and molecular ratios** observed in the Orion hot core region and our model, M7, calculations. The table also lists times of best fit. Apart from CH_2DOH our model seems to be consistent with the observations reported by Neill et al. (2013a,b).

4.2 Comparison with previous astrochemical modelling

In this section, we also briefly compare our model results with other astrochemical modelling efforts. Albertsson et al. (2013) performed a detailed chemical study of deuterated molecules using gas-grain chemical models. They estimate

Table 5. The calculated deuterium fractional abundances and molecular D/H ratios in hot core Model M7 (Phase II) in comparison with observations of the Orion KL hot core.

Species	Observations	This Work M7	Time of best fit yrs	Ref
HDO	~ 4.5 (-8)	≥ 4.2 (-8)	≥ 3.8 (4)	Neill et al. (2013a)
NH₂D	1.4 (-8)	≥ 1 (-8)	0.3 - 5.8 (5)	Neill et al. (2013b)
HD₂CO	2.9 (-10)	~ 1 (-10)-3 (-8)	≥ 1.3 (4)	Neill et al. (2013b)
CH₃OD	1.9 (-9)	≤ 1 (-10)	all times	Neill et al. (2013b)
CH₂DOH	4.5 (-9)	≤ 1 (-10)	all times	Neill et al. (2013b)
Ratio				
HDO/H₂O	$\sim 3^{+3.1}_{-1.7}$ (-3)	1.3-6 (-3)	1.6-8.9 (5)	Neill et al. (2013a)
NH₂D/NH₃	$\sim 6.8 \pm 2.4$ (-3)	4.5-9.2 (-3)	1.5-1.9 (4)	Neill et al. (2013b)
HD₂CO/H₂CO	≤ 0.005	~ 5 (-3)	1.05-1.15 (5)	Neill et al. (2013b)
CH₃OD/CH₃OH	≤ 1.8 (-3)	≤ 1.8 (-3)	≥ 4.92 (5)	Neill et al. (2013b)
CH₂DOH/CH₃OH	≤ 4.2 (-3)	≤ 4.2 (-3)	≥ 3.29 (5)	Neill et al. (2013b)

a(b) means $a \times 10^b$

the abundances of HDO in hot cores and corinos to be $\sim 10^{-7}$. This value best fits our models for times around $1-5 \times 10^5$ yrs for hot corinos (e.g. Fig. 1-a) and time ranges of $10^{5.2}-10^6$ yrs, and $10^{4.3}-10^6$ yrs for hot cores of 5 and $25 M_{\odot}$, respectively.

Aikawa et al. (2012) used a gas-grain chemical model of an in-falling parcel of fluid to study the evolution of deuterated species and the deuterium fragmentation from pre- to proto-stellar cores. They found that as the gas depletion increases, the deuterium fraction enhances. Our calculations for both hot corinos, Model M3, and hot cores, Models M6 and M9, showed that for most of the studied species in both environments, the fractional abundances are enhanced as the gas depletion percentage increases; see Figs. (3 and 4). These results are supported by the model calculations of Aikawa et al. (2012).

5 CONCLUSION

We modelled the deuterium chemistry in hot corinos and cores using an extended, updated and improved version of the chemical model used by Viti et al. (2004) for hot cores and modified for hot corinos as described in Awad et al. (2010). Unlike previous studies, here we focus on the proto-stellar phase where the evaporation of mantle species occurs and influences the chemistry of the core. The novelty of our approach is the treatment of the evaporation of deuterated species adopting the experimental results of Collings et al. (2003a, 2004). We studied the influence of varying the physical conditions of star forming regions, namely the density and depletion efficiency, on the chemical evolution of the core. In addition, we explored the effect of changing the collapse timescale of low-mass stellar cores, as well as the final mass of the protostar.

For both hot core and corino environments, we found that lowering the depletion percentage decreases the abundance of most of the studied deuterated species, with the exception of HD₂CO in both cores and D₂CO in hot cores. Deuterated species in hot cores are more sensitive to the changes in the cores density than in hot corinos. Gener-

ally, we find that decreasing the density of the gas reduces the abundances of the deuterated species, in particular large species, in hot cores more than in hot corinos.

In addition, in hot corinos, our models showed that the collapse time affects the abundance of HD₂CO, NH₂D, CH₂DOH, and HDO, so that this should also be taken into account when attempting to model the deuteration of water, besides taking into account variations in physical parameters and dust temperature as already explored by Taquet et al. (2012) and Cazaux et al. (2011).

Our model failed to reproduce the observed abundances of large organic species such as HCOOCH₃, and its deuterated counterpart. This is most likely due to an incomplete surface chemistry as well as the lack of multiply deuterated species in our chemical network.

ACKNOWLEDGMENTS

Z.Awad is grateful to Professor C. Ceccarelli for her helpful suggestions to improve the results and discussion part. E. Bayet thanks STFC astrophysics at Oxford 2010-2015 (ref: ST/H002456/1) and John Fill OUP research fund "Molecules in galaxies: securing Oxford's position in the ALMA era" (ref: 0921267). The research leading to these results has received funding from the (European Community's) Seventh Framework Program [FP7/20072013] under grant agreement no. 238258. P. Caselli acknowledges the financial support of the European Research Council (ERC; project PALs 320620). S. Viti and P. Caselli acknowledge support the UK Science and Technology Funding Council.

REFERENCES

- Aikawa Y., Wakelam V., Hersant F., Garrod R. T., Herbst E., 2012, ApJ, 760, 40
- Albertsson T., Semenov D. A., Vasyunin A. I., Henning T., Herbst E., 2013, ApJS, 207, 27
- André P., Ward-Thompson D., Barsony M., 1993, ApJ, 406, 122

- Awad Z., 2010, PhD thesis, Physics and Astronomy Department, UCL
- Awad Z., Viti S., Collings M. P., Williams D. A., 2010, *MNRAS*, p. 1006
- Bacmann A., Lefloch B., Ceccarelli C., Steinacker J., Castets A., Loinard L., 2003, *ApJ Letter*, 585, L55
- Bergin E. A., Cleeves L. I., Gorti U., Zhang K., Blake G. A., Green J. D., Andrews S. M., Evans II N. J., Henning T., Öberg K., Pontoppidan K., Qi C., Salyk C., van Dishoeck E. F., 2013, *Nature*, 493, 644
- Bertoldi F., Timmermann R., Rosenthal D., Drapatz S., Wright C. M., 1999, *A&A*, 346, 267
- Brown P. D., Millar T. J., 1989a, *MNRAS*, 237, 661
- Brown P. D., Millar T. J., 1989b, *MNRAS*, 240, 25
- Butner H. M., Charnley S. B., Ceccarelli C., Rodgers S. D., Pardo J. R., Parise B., Cernicharo J., Davis G. R., 2007, *ApJ Letter*, 659, L137
- Butner H. M., Loren R. B., 1988, in *Bulletin of the American Astronomical Society Vol. 20 of Bulletin of the American Astronomical Society, A Survey of DCO⁺ in Low Mass Molecular Cores*. p. 956
- Caselli P., Ceccarelli C., 2012, *The Astronomy and Astrophysics Review*, 20, 56
- Caselli P., van der Tak F. F. S., Ceccarelli C., Bacmann A., 2003, *A&A*, 403, L37
- Caselli P., Walmsley C. M., Zucconi A., Tafalla M., Dore L., Myers P. C., 2002, *ApJ*, 565, 344
- Caux E., Ceccarelli C., Pagani L., Maret S., Castets A., Pardo J. R., 2002, *A&A*, 383, L9
- Cazaux S., Caselli P., Spaans M., 2011, *ApJ Letter*, 741, L34
- Ceccarelli C., Caselli P., Herbst E., Tielens A. G. G. M., Caux E., 2007, in Reipurth B., Jewitt D., Keil K., eds, *Protostars and Planets V Extreme Deuteration and Hot Corinos: The Earliest Chemical Signatures of Low-Mass Star Formation*. pp 47–62
- Ceccarelli C., Castets A., Loinard L., Caux E., Tielens A. G. G. M., 1998, *A&A*, 338, L43
- Ceccarelli C., Loinard L., Castets A., Tielens A. G. G. M., Caux E., Lefloch B., Vastel C., 2001, *A&A*, 372, 998
- Chen H.-R., Liu S.-Y., Su Y.-N., Wang M.-Y., 2011, *ApJ*, 743, 196
- Collings M. P., Anderson M. A., Chen R., Dever J. W., Viti S., Williams D. A., McCoustra M. R. S., 2004, *MNRAS*, 354, 1133
- Collings M. P., Dever J. W., Fraser H. J., McCoustra M. R. S., Williams D. A., 2003a, *ApJ*, 583, 1058
- Coutens A., Vastel C., Cazaux S., Bottinelli S., Caux E., Ceccarelli C., Demyk K., Taquet V., Wakelam V., 2013, *A&A*, 553, A75
- Crapsi A., Caselli P., Walmsley C. M., Myers P. C., Tafalla M., Lee C. W., Bourke T. L., 2005, *ApJ*, 619, 379
- Demyk K., Bottinelli S., Caux E., Vastel C., Ceccarelli C., Kahane C., Castets A., 2010, *A&A*, 517, A17
- Ehrenfreund P., Charnley S. B., 2000, *Annu. Rev. A&A*, 38, 427
- Emprechtinger M., Caselli P., Volgenau N. H., Stutzki J., Wiedner M. C., 2009, *A&A*, 493, 89
- Flower D. R., Pineau Des Forêts G., Walmsley C. M., 2006, *A&A*, 449, 621
- Fontani F., Caselli P., Bourke T. L., Cesaroni R., Brand J., 2008, *A&A*, 477, L45
- Fontani F., Caselli P., Crapsi A., Cesaroni R., Molinari S., Testi L., Brand J., 2006, *A&A*, 460, 709
- Garrod R. T., Weaver S. L. W., Herbst E., 2008, *ApJ*, 682, 283
- Gerin M., Combes F., Wlodarczak G., Encrenaz P., Laurent C., 1992, *A&A*, 253, L29
- Gerlich D., Herbst E., Roueff E., 2002, *Planetary and Space Science*, 50, 1275
- Henkel C., Mauersberger R., Wilson T. L., Snyder L. E., Menten K. M., Wouterloot J. G. A., 1987, *A&A*, 182, 299
- Herbst E., van Dishoeck E. F., 2009, *Annu. Rev. A&A*, 47, 427
- Hugo E., Asvany O., Schlemmer S., 2009, *J. Chem. Phys.*, 130, 164302
- Jacq T., Walmsley C. M., Mauersberger R., Anderson T., Herbst E., De Lucia F. C., 1993, *A&A*, 271, 276
- Kaufman M. J., Hollenbach D. J., Tielens A. G. G. M., 1998, *ApJ*, 497, 276
- Linsky J. L., Diplas A., Wood B. E., Brown A., Ayres T. R., Savage B. D., 1995, *ApJ*, 451, 335
- Loren R. B., Wootten A., 1985, *ApJ*, 299, 947
- McElroy D., Walsh C., Markwick A. J., Cordiner M. A., Smith K., Millar T. J., 2013, *A&A*, 550, A36
- Millar T. J., 2005, *Astronomy and Geophysics*, 46, 020000
- Millar T. J., Bennett A., Herbst E., 1989, *ApJ*, 340, 906
- Millar T. J., Roberts H., Markwick A. J., Charnley S. B., 2000, in *Astronomy, physics and chemistry of H⁺₃* Vol. 358 of *Royal Society of London Philosophical Transactions Series A, The role of H₂D⁺ in the deuteration of interstellar molecules*. p. 2535
- Neill J. L., Crockett N. R., Bergin E. A., Pearson J. C., Xu L.-H., 2013b, *ApJ*, 777, 85
- Neill J. L., Wang S., Bergin E. A., Crockett N. R., Favre C., Plume R., Melnick G. J., 2013a, *ApJ*, 770, 142
- Neufeld D. A., Green J. D., Hollenbach D. J., Sonnentrucker P., Melnick G. J., Bergin E. A., Snell R. L., Forrest W. J., Watson D. M., Kaufman M. J., 2006, *ApJ Letter*, 647, L33
- Oliveira C. M., Hébrard G., Howk J. C., Kruk J. W., Chayer P., Moos H. W., 2003, *ApJ*, 587, 235
- Parise B., Castets A., Herbst E., Caux E., Ceccarelli C., Mukhopadhyay I., Tielens A. G. G. M., 2004, *A&A*, 416, 159
- Parise B., Ceccarelli C., Tielens A. G. G. M., Herbst E., Lefloch B., Caux E., Castets A., Mukhopadhyay I., Pagani L., Loinard L., 2002, *A&A*, 393, L49
- Parise B., Leurini S., Schilke P., Roueff E., Thorwirth S., Lis D. C., 2009, *A&A*, 508, 737
- Penzias A. A., 1979, *ApJ*, 228, 430
- Pillai T., Caselli P., Kauffmann J., Zhang Q., Thompson M. A., Lis D. C., 2012, *ApJ*, 751, 135
- Polehampton E. T., Baluteau J., Ceccarelli C., Swinyard B. M., Caux E., 2002, *A&A*, 388, L44
- Rawlings J. M. C., Hartquist T. W., Menten K. M., Williams D. A., 1992, *MNRAS*, 255, 471
- Roberts H., Herbst E., Millar T. J., 2003, *ApJ Letter*, 591, L41
- Roberts H., Herbst E., Millar T. J., 2004, *A&A*, 424, 905
- Roberts H., Millar T. J., 2000a, *A&A*, 361, 388
- Roberts H., Millar T. J., 2000b, *A&A*, 364, 780
- Roberts H., Millar T. J., 2007, *A&A*, 471, 849
- Rodgers S. D., Millar T. J., 1996, *MNRAS*, 280, 1046

- Rodriguez Kuiper E. N., Kuiper T. B. H., Zuckerman B., 1978, *ApJ Letter*, 219, L49
- Roueff E., Gerin M., Lis D. C., Wootten A., Marcelino N., Cernicharo J., Tercero B., 2013, *Journal of Physical Chemistry A*, 117, 9959
- Roueff E., Tiné S., Coudert L. H., Pineau des Forêts G., Falgarone E., Gerin M., 2000, *A&A*, 354, L63
- Saito S., Mikami H., Yamamoto S., Murata Y., Kawabe R., 1994, in Ishiguro M., Welch J., eds, *IAU Colloq. 140: Astronomy with Millimeter and Submillimeter Wave Interferometry Vol. 59 of Astronomical Society of the Pacific Conference Series, Aperture Synthesis Maps of NH₂D and CH₃OD Lines toward Orion-KL: The Origin of NH₃ and CH₃OH*. p. 241
- Sakai N., Sakai T., Hirota T., Yamamoto S., 2008, *ApJ*, 672, 371
- Sakai N., Sakai T., Hirota T., Yamamoto S., 2009, *ApJ*, 702, 1025
- Shah R. Y., Wootten A., 2001, *ApJ*, 554, 933
- Sipilä O., Hugo E., Harju J., Asvany O., Juvela M., Schlemmer S., 2010, *A&A*, 509, A98
- Stark R., Sandell G., Beck S. C., Hogerheijde M. R., van Dishoeck E. F., van der Wal P., van der Tak F. F. S., Schäfer F., Melnick G. J., Ashby M. L. N., de Lange G., 2004, *ApJ*, 608, 341
- Stark R., van der Tak F. F. S., van Dishoeck E. F., 1999, *ApJ Letter*, 521, L67
- Taquet V., Ceccarelli C., Kahane C., 2012, *A&A*, 538, A42
- Tielens A. G. G. M., 1983, *A&A*, 119, 177
- Tielens A. G. G. M., 2013, *Reviews of Modern Physics*, 85, 1021
- Tielens A. G. G. M., Hagen W., 1982, *A&A*, 114, 245
- Tiné S., Roueff E., Falgarone E., Gerin M., Pineau des Forêts G., 2000, *A&A*, 356, 1039
- Turner B. E., 1990, *ApJ Letter*, 362, L29
- van der Tak F. F. S., Schilke P., Müller H. S. P., Lis D. C., Phillips T. G., Gerin M., Roueff E., 2002, *A&A*, 388, L53
- van Dishoeck E. F., Blake G. A., Jansen D. J., Groesbeck T. D., 1995, *ApJ*, 447, 760
- Vastel C., Phillips T. G., Ceccarelli C., Pearson J., 2003, *ApJ Letter*, 593, L97
- Vastel C., Phillips T. G., Yoshida H., 2004, *ApJ Letter*, 606, L127
- Viti S., Collings M. P., Dever J. W., McCoustra M. R. S., Williams D. A., 2004, *MNRAS*, 354, 1141
- Viti S., Williams D. A., 1999, *MNRAS*, 305, 755
- Vrtilek J. M., Gottlieb C. A., Langer W. D., Thaddeus P., Wilson R. W., 1985, *ApJ Letter*, 296, L35
- Walmsley C. M., Flower D. R., Pineau des Forêts G., 2004, *A&A*, 418, 1035
- Watanabe N., Shiraki T., Kouchi A., 2003, *ApJ Letter*, 588, L121
- Watson W. D., 1980, in *Les Spectres des Molécules Simples au Laboratoire et en Astrophysique Chemical reactions at the surfaces of interstellar dust grains*. pp 526–544
- Wilson R. W., Penzias A. A., Jefferts K. B., Solomon P. M., 1973, *ApJ Letter*, 179, L107
- Woodall J., Agúndez M., Markwick-Kemper A. J., Millar T. J., 2007, *A&A*, 466, 1197
- Wright C. M., van Dishoeck E. F., Cox P., Sidher S. D., Kessler M. F., 1999, *ApJ Letter*, 515, L29
- Yuan Y., Neufeld D. A., Sonnentrucker P., Melnick G. J., Watson D. M., 2012, *ApJ*, 753, 126

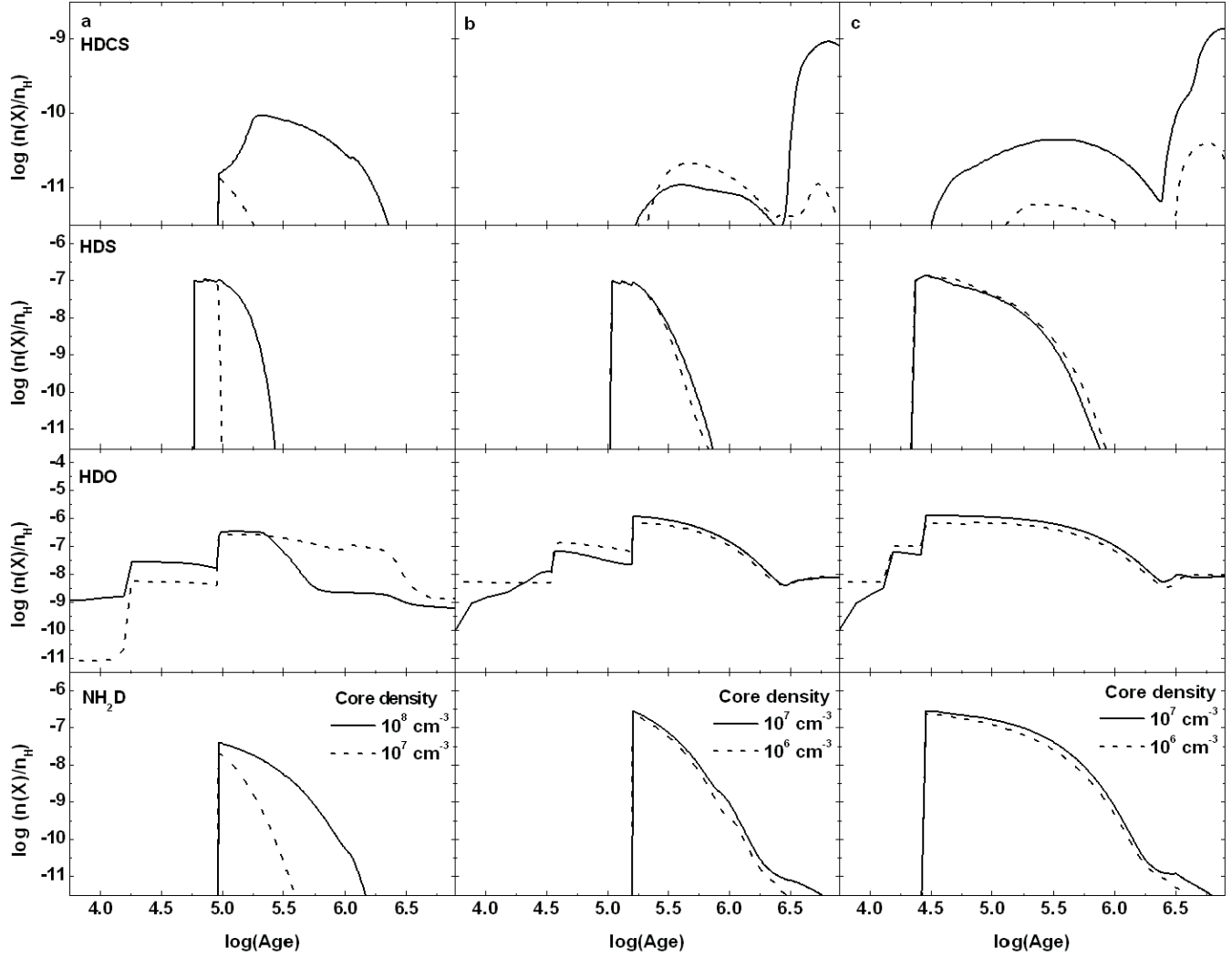


Figure 1. The chemical evolution (from top to bottom) of HDCS, HDS, HDO, and NH_2D in hot corinos (panel a: 1 M_\odot) and hot cores (panel b: 5 M_\odot , and panel c: 25 M_\odot) as a function of time, for Phase II calculations. The different curves compare the evolution of the species at two different final densities for the collapsing cloud (see key in bottom plots, and Table 3).

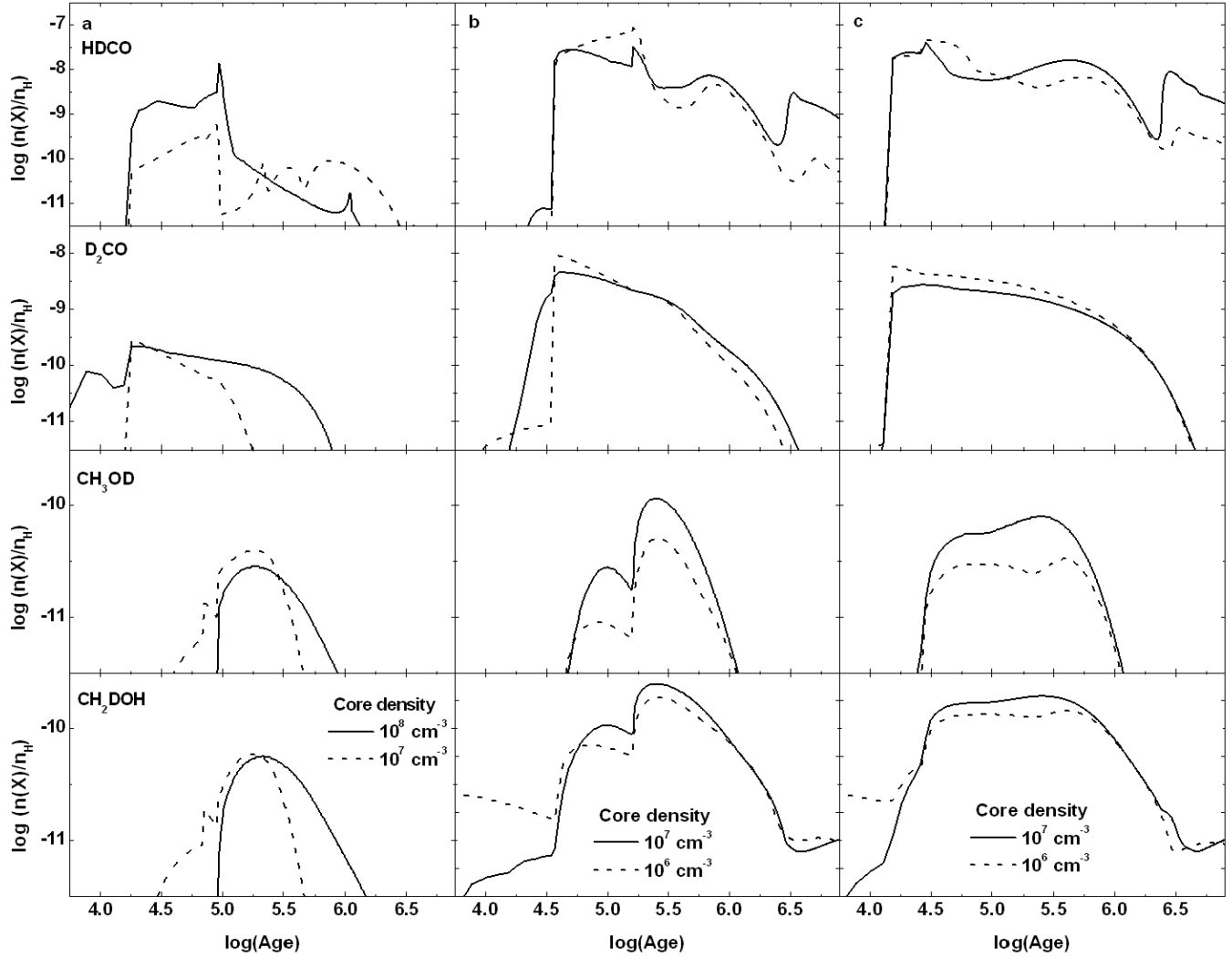


Figure 2. Similar to Fig. 1 but for deuterated formaldehyde and methanol (see key).

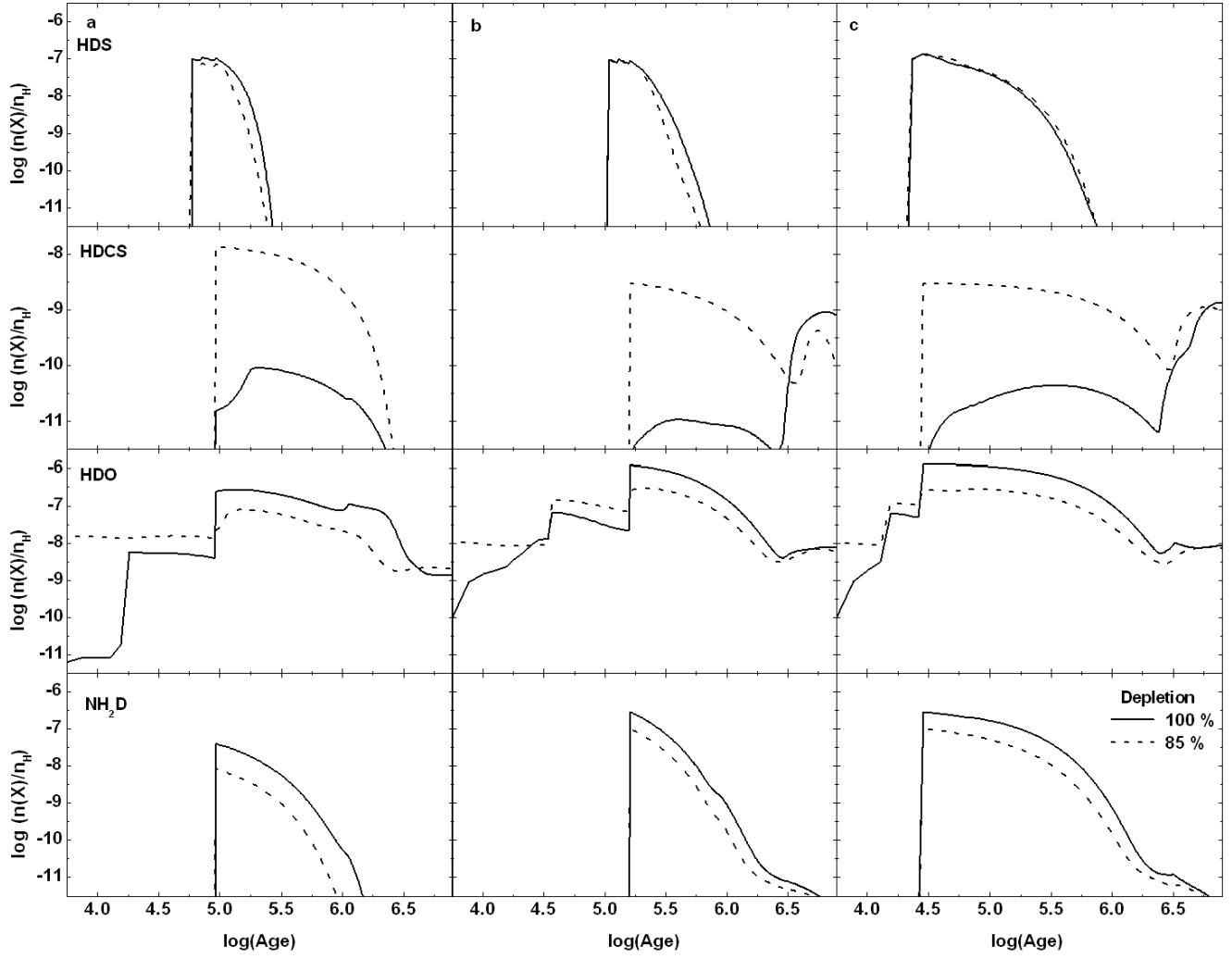


Figure 3. Chemical evolution of HDCS, HDS, HDO, and NH_2D as a function of time, during Phase II, at different depletion on grain surfaces (see key text in bottom right plot, and Table 3) for different cores: (a) $1 M_\odot$, (b) $5 M_\odot$, and (c) $25 M_\odot$.

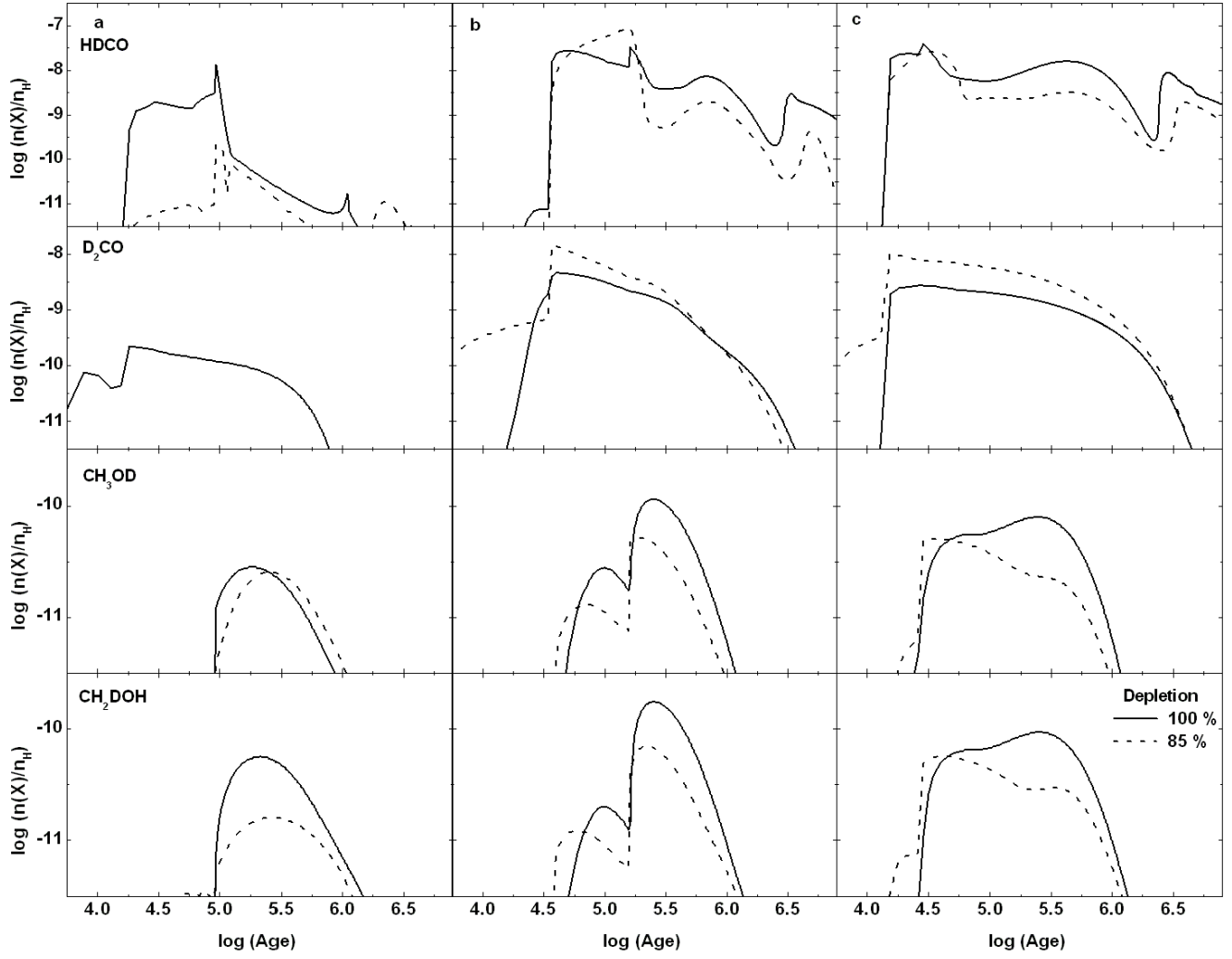


Figure 4. Similar to Fig. 3 but for deuterated organic species (see key).

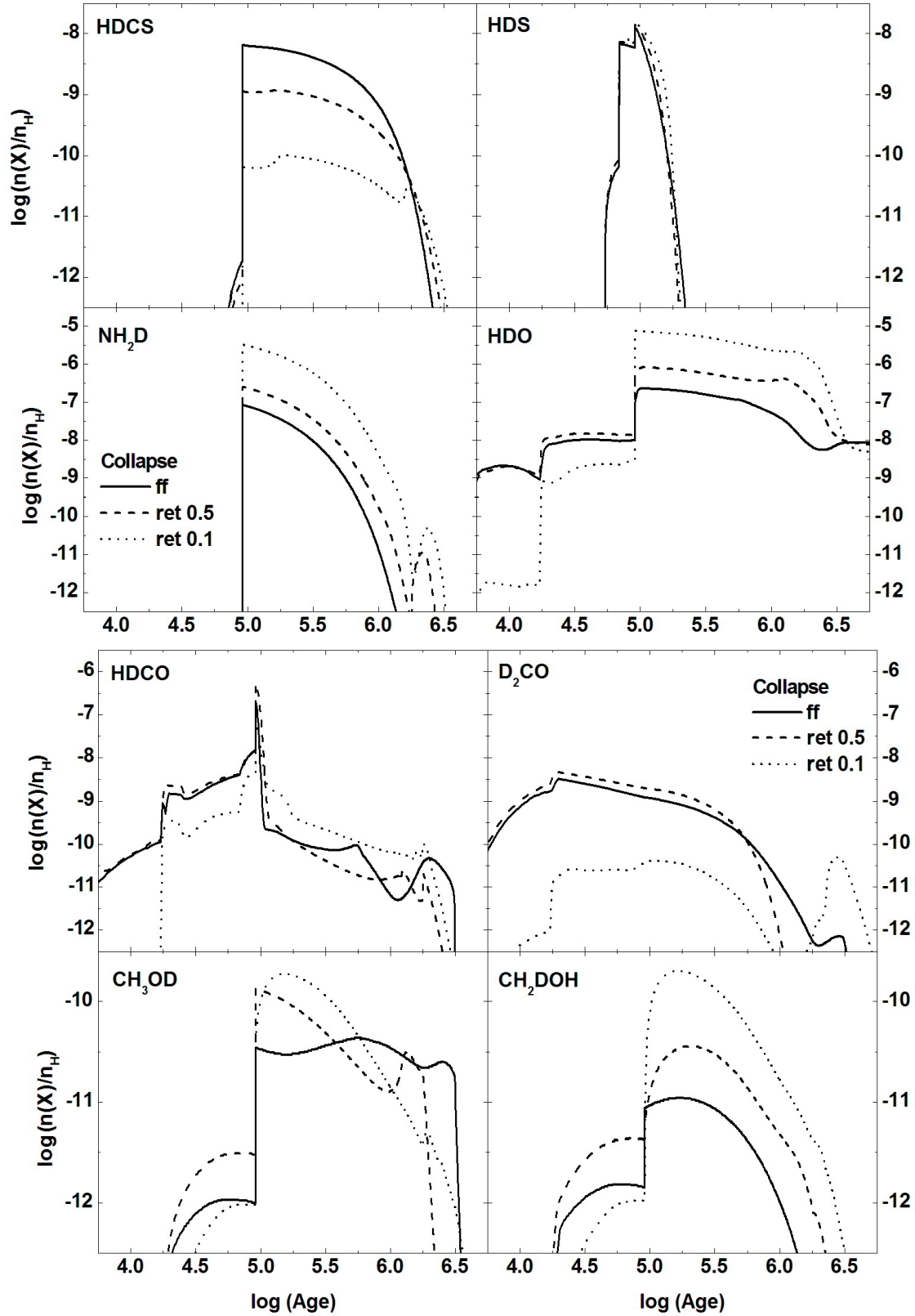


Figure 5. Chemical evolution of a selected set of deuterated species during the the warming-up phase (Phase II) as a function of time using different collapsing modes: the free fall (ff: solid line), retarded; 0.5ff speed (ret 0.5: dashed line) and 0.1ff speed (ret 0.1: dotted line), see key and Table 3.

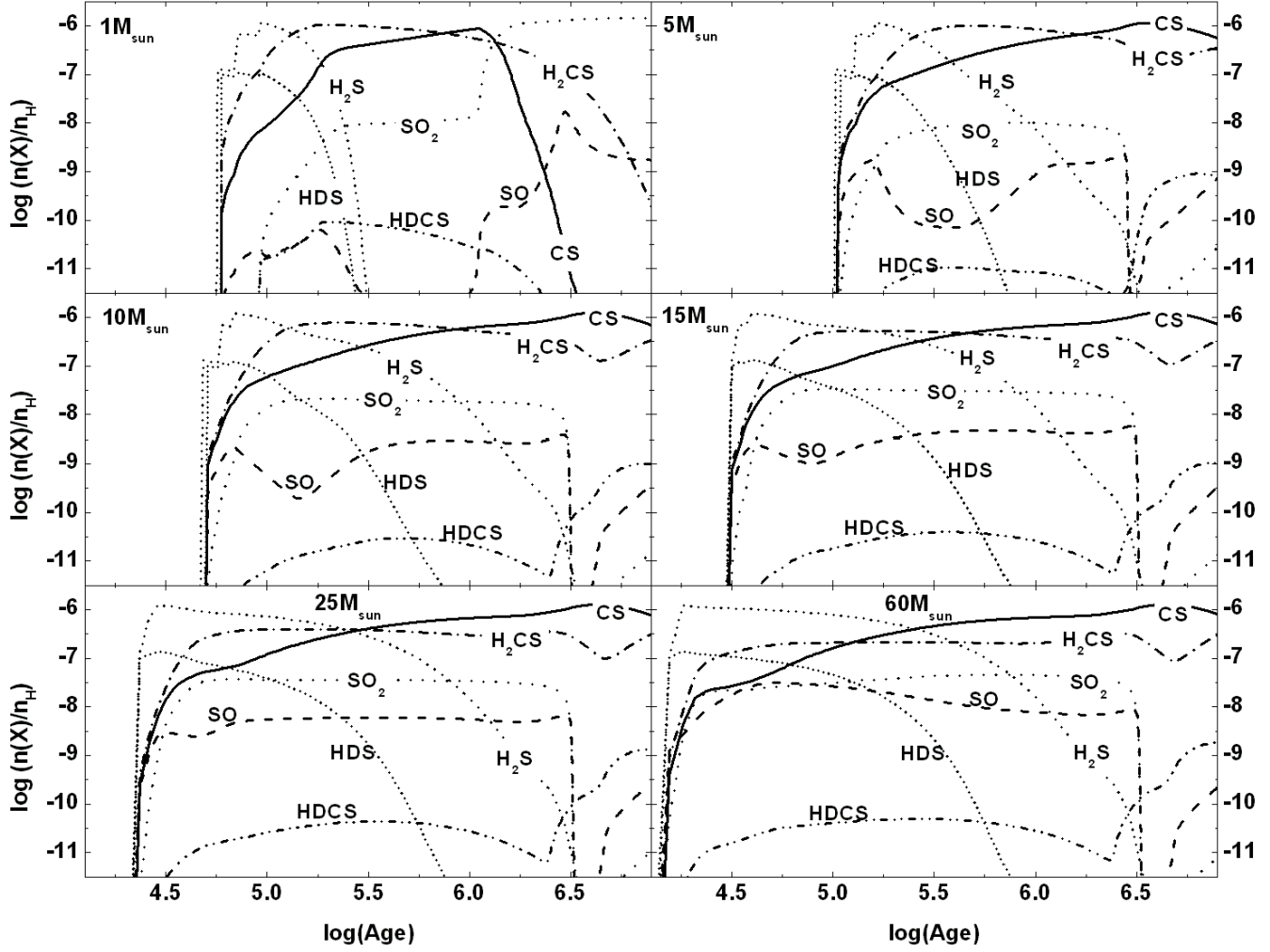


Figure 6. The chemical evolution of S-bearing species and their deuterated counterparts as a function of time in warm and hot cores for various masses as indicated on the plots (upper left corners). The fractional abundances of the studied species are represented by different line styles.